Volume 9, Number 2
1009-1963/2000/09(02)/0113-06
CHINESE PHYSICS
February, 2000
© 2000 Chin. Phys. Soc.

LOCAL MODE SPECTROSCOPIC STUDY OF THE AsH_3 MOLECULE: THE PERTURBED (500) LOCAL MODE OVERTONE*

Lin Hai(林 海)[a], Oleg N. Ulenikov[a)b)], Igor M. Olekhnovitch[a)b)],
Wang Dong(王 冬)[a], Chen Xi-yi(陈习意)[a], Hao Lu-yuan(郝绿原),
and Zhu Qing-shi(朱清时)[a]

[a] *Laboratory of Bond Selective Chemistry, University of Science and Technology of China, Hefei* 230026, *China*

[b] *Laboratory of Molecular Spectroscopy, Department of Physics, Tomsk State University, Tomsk* 634050, *Russia*

(Received 16 April 1999)

The high resolution Fourier transform spectra of AsH_3 in the region of 9720–9900 cm^{-1}, which had been recorded at a resolution of 0.015 cm^{-1}, were assigned to the (500; A_1) and (500; E) local mode overtones and rotationally analyzed. The effective spectroscopic parameters were obtained by nonlinear least-squares fitting the vibration-rotational Hamiltonian with the rotational energy levels up to $J = 6$ (98 levels in all) included. The evolution of the rotational energy patterns from $v = 1$ to $v = 6$ shows that the tendency of normal mode to local mode vibration evolution has been stopped by perturbations in relatively high energy region.

PACC: 3380

I. INTRODUCTION

In the past ten years, a lot of work has been done theoretically[1−7] as well as experimentally[8−14] to investigate the local mode effects on the rotational energy level structure of stretching overtone states in some small symmetrical molecules. In the local mode limit the theory has predicted the disappearance of Coriolis effects on the rotational energy levels and simple relationships between the parameters of the vibrationally diagonal and off-diagonal H_{22} terms.[2−7] These predictions are found to be closely satisfied in some XH_n-type molecules.[8−15] The most striking result is the early experimental observation of the symmetric top parallel band structure of the stretching overtone states in spherical top molecules.[8]

AsH_3 is a nice molecule to study the local mode effects because it is close to the local mode limit. A medium resolution spectroscopic study of AsH_3 in the region of 1800–8000 cm^{-1} was done and an anharmonically coupled anharmonic oscillators (ACAO) model was successfully used both to explain and to predict the stretching vibrational spectra in Ref.[16]. Later, a vibrational calculation taking into account Fermi resonance interactions between stretching and bending states was proposed by Lukka et al.[17]. Recently, much experimental work on high resolution spectroscopic study of AsH_3 were reported[18−20] and the stretching potential surface was improved by the ACAO model with these high resolution results included in the fitting.[18] However, it needs to be mentioned that no high resolution spectroscopic study of the forth stretching overtone manifold has been so far reported, because of the quite weak absorptions in the region. We present here a detailed high resolution Fourier transform spectroscopic study of the (500) local mode overtone.

II. EXPERIMENTAL ARRANGEMENT

Arsine was purchased from Nanjing special gas company with a stated purity of 99.99%. The high resolution Fourier transform spectrum was recorded on a Bruker IFS120 HR spectrometer, which was equipped with a tungsten lamp source, a Si/CaF_2 beamsplitter and a Si diode detector. The focal length of the collimate mirror is 418 mm. Proper electronic filters were used to control the bandwidth of the detector output and to reduce electronic noises. A White-type multipass cell was adjusted to a path length of 105 m in order to record the weak local mode overtones. The sample pressure was 12600 Pa, and was measured and monitored by a capacitance manometer of 0.5% full-scale accuracy. The laboratory was air-conditioned and the temperature was (23±2)°C. The aperture diameter was 1.15 mm and the acquisition mode was single-sided, fast return. A double-sided interferogram was recorded at a resolution of 256 cm^{-1} for phase correction with the Mertz method. The apodization function was of the Norton-Beer-Weak type. One hundred and fifty separate spectra were obtained, each resulting from 25 co-added scans. Then the 150 spectra

* Project supported by the National Natural Science Foundation of China (Grant No. 29573120), the National Natural Science Youth Foundation of China (Grant Nos. 29903010 and GG0366) and the Chinese Academy of Sciences (Grant No. KJ951-A1-510).

which amount to 3750 scans in all were averaged point by point to improve the signal to noise ratio. The precision of the spectrum was estimated to be better than $0.002\,\mathrm{cm}^{-1}$ for strong lines and 0.007 cm^{-1} for weak lines. The interferometer and its optics were kept under a vacuum of 2 Pa during the experiment. Calibration was carried out with the lines of residual water taking from Ref.[20]. The accuracy of the calibration was better than $0.002\,\mathrm{cm}^{-1}$.

The spectra ranging from 9600 to $12000\,\mathrm{cm}^{-1}$ were covered. The region from 9720 to $9900\,\mathrm{cm}^{-1}$ was assigned to the (500) overtone, which consisted of the (500; A_1) band and (500; E) band, according to the local mode vibrational analysis.[16] The local mode notation ($n_1n_2n_3$) used to label the excited stretching overtone states gave the quantum number of excitation in the three individual As-H bonds in the local mode limit, assuming that only As-H stretching vibrations were excited. In some cases, we added a C_{3v} symmetry species label, such as (500; E), etc. The (410) combinational band systems located at $10145\,\mathrm{cm}^{-1}$ were also observed, so far as we know, for the first time.

Ⅲ. THE VIBRATIONAL-ROTATIONAL MATRIX ELEMENTS

A local mode calculation shows that the $(500; A_1)$ and $(500; E)$ bands are degenerated and are coupled by the Darling-Dennison interactions.[1] As a result, in order to interpret the complicated rotational pattern of the upper states, the $(500; A_1)$ and $(500; E)$ bands at $9841\,\mathrm{cm}^{-1}$ which are close to each other must be analyzed simultaneously. The model used here is the same as that used for the interacting A_1 and E stretching fundamentals.[9,22] The diagonal matrix elements for the ground state and for the A_1 states take the conventional form

$$\begin{aligned} H_{\mathrm{s}} = \langle v; JK|H|v; JK\rangle =& G_{\mathrm{s}} + B_{\mathrm{s}}[J(J+1) - K^2] + C_{\mathrm{s}}K^2 \\ & - D^{\mathrm{s}}_J J^2(J+1)^2 - D^{\mathrm{s}}_{JK} J(J+1)K^2 - D^{\mathrm{s}}_K K^4 + \cdots \end{aligned} \tag{1}$$

The corresponding expression for the E states takes the form

$$\begin{aligned} H_{\mathrm{t}} = \langle vl; JK|H|vl; JK\rangle =& G_{\mathrm{t}} + B_{\mathrm{t}}[J(J+1) - K^2] + C_{\mathrm{t}}K^2 \\ & - (C\zeta)_{\mathrm{t}}Kl - D^{\mathrm{s}}_J J^2(J+1)^2 - D^{\mathrm{s}}_{JK} J(J+1)K^2 - D^{\mathrm{s}}_K K^4 \\ & + \eta^{\mathrm{t}}_J J(J+1)Kl + \eta^{\mathrm{t}}_K K^3 + \cdots \end{aligned} \tag{2}$$

In these equations, the basis function is a product of vibrational eigenfunctions and symmetric top rigid rotor eigenfunctions. J and l are, respectively, total angular momentum and vibrational angular momentum quantum numbers; K is the component of J along the molecular axis and $K = |k|$. $|E^+\rangle$ and $|E^-\rangle$ denote doubly degenerate E state with different vibrational angular momentum quantum numbers $l = +1$ and $l = -1$.

The Coriolis interaction between the E and A_1 bands takes the form

$$\begin{aligned} &\langle 500E^+; JK+1|H_{21}|500A_1; JK\rangle \\ &= -\langle 500A_1; JK+1|H_{21}|500E^-; JK\rangle \\ &= \sqrt{2}B\Omega\zeta^y_{\mathrm{eff}}F(J,K), \end{aligned} \tag{3}$$

where $F(J,K) = \sqrt{J(J+1) - K(K+1)}$.

All H_{22} operators are included in our model. Specifically, the l- and r-resonance terms couple the different vibrational angular momentum states in the E vibrational band. The l-resonance matrix elements are

$$\begin{aligned} &\langle 500E^+; JK+2|H_{22} + H_{24}|500E^-; JK\rangle \\ &= -\frac{1}{2}[q_{\mathrm{eff}} + q^J_{\mathrm{eff}}J(J+1)]F(J,K)F(J,K+1), \end{aligned} \tag{4}$$

and the r-resonance matrix element is

$$\begin{aligned} &\langle 500E^-; JK+1|H_{22}|500E^+; JK\rangle \\ &= 2r_{\mathrm{eff}}(2K+1)F(J,K). \end{aligned} \tag{5}$$

The other two H_{22} operators, the α-resonance terms, have also been included. They couple the rotational levels of the $(500; A_1)$ and $(500; E)$ vibrational states. The corresponding matrix elements are

$$\begin{aligned} &\langle 500E^-; JK+2|H_{22} + H_{24}|500A_1; JK\rangle \\ &= \langle 500A_1; JK+2|H_{22} + H_{24}|500E^+; JK\rangle \\ &= \frac{\sqrt{2}}{4}\Big[\alpha^{BB}_{\mathrm{eff}} + \alpha^{BB,J}_{\mathrm{eff}}J(J+1) \\ &\quad + \alpha^{BB,K}_{\mathrm{eff}}(K^2 + (K+2)^2)\Big]F(J,K)F(J,K+1). \end{aligned} \tag{6}$$

and

$$\begin{aligned}&\langle 500E^+; JK+1|H_{22}+H_{24}|600A_1; JK\rangle\\ &=\langle 500A_1; JK+1|H_{22}+H_{24}|500E^-; JK\rangle\\ &=\frac{\sqrt{2}}{4}[\alpha_{\rm eff}^{BC}+\alpha_{\rm eff}^{BC,J}J(J+1)](2K+1)\\ &\quad\times F(J,K)F(J,K+1). \qquad (7)\end{aligned}$$

It needs to be particularly noticed that all these vibration-rotational parameters are effective and not related in a simple fashion to the corresponding parameters obtained from the analysis of the stretching fundamental bands.

IV. ROTATIONAL ANALYSIS

Parts of the spectra of the $(500; A_1)$ and $(500; E)$ bands are illustrated in Fig.1. The label $\Gamma_{\rm v} : J''K''\Gamma_{\rm r}'' - \Gamma_{\rm v} : J'K'\Gamma_{\rm r}'$ denotes the transition from ground state level to upper state level, where $\Gamma_{\rm v}$ is the symmetry species of the vibrational state and $\Gamma_{\rm r}$ is the symmetry species of the vibrational-rotational level. The transitions were assigned by means of ground state combination differences (GSCD). The ground state energy levels are obtained from Ref.[23]. The spectroscopic parameters listed in Table 1 are obtained by nonlinear least-squares fitting, and the upper state energy levels obtained from the assigned lines (Table 2).

No K structure is found in this complicated spectrum. Combination differences with three allowed transitions (of the P, Q and R branches) cannot be satisfied for most of the upper levels of the $(500; A_1)$ and $(500; E)$ bands, instead, only two of the allowed transitions are found. Forbidden transitions of $\Delta K = 0, 2$ and 3 for $(500; A_1)$ band and/or for $(500; E)$ band are found at the same time.

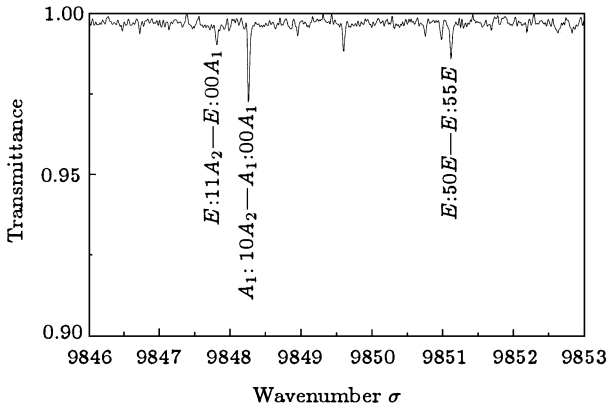


Fig.1. Part of the expanded picture of the (500) overtone of AsH_3. The label $\Gamma_{\rm v} : J''K''\Gamma_{\rm r}'' - \Gamma_{\rm v} : J'K'\Gamma_{\rm r}'$ denotes the transition from ground state level (single primed) to upper state level (double primed), where $\Gamma_{\rm v}$ is the vibrational symmetry and $\Gamma_{\rm r}$ is the vibrational-rotational symmetry.

In fact, it is difficult to assign the J and K quantum numbers for the upper levels due to the mixing of wavefunctions. The low J energy levels with $K = 0$ and $K = 1$ are firstly assigned, and the v_0, B and C parameters optimized. Secondly, these parameters are used to predict other upper state energy levels. Then more lines are assigned and more levels are added to the fitting to give higher order parameters. The procedure is repeated till the transitions up to $J = 6$ are assigned. For some upper levels, since no combination differences can be found at all, we use the calculated value to assign the observed transitions.

In our analysis, most of the strong lines were assigned. It is interesting to find that the intensities of some forbidden transitions are strong in contrast with those transitions normally allowed. When J is higher than 6, it is difficult for us to determine one from a lot of pairs of lines satisfying the combination differences as a result of high density of lines in the Q and R branches. The spectroscopic parameters which were obtained by least-squares fitting are listed in Table 1. Table 2 demonstrates the calculated and observed rotational energy levels up to $J = 6$ for the $(500; A_1)$ state (33 levels in all) and $(500; E)$ state (65 levels in all). The number of transitions found by ground state combination differences for each energy level is also given in the last column. The standard deviation of the fit is $0.03\,{\rm cm}^{-1}$, which is satisfactory compared with the experimental uncertainty of $0.015\,{\rm cm}^{-1}$. Some high order parameters, e.g., $\zeta_{\rm eff}^{y}$, $q_{\rm eff}^{K}$, $r_{\rm eff}^{J}$ and $\alpha_{\rm eff}^{BC,K}$ cannot be significantly determined and are fitted to zero in our analysis. It is easy to see that the obtained parameters have successfully reproduced the upper state levels.

Table 1. Spectroscopic parameters ($\rm cm^{-1}$) for the (500) local mode overtone of AsH_3.

Parameter	$\langle 500; A_1\|500; A_1\rangle$	$\langle 500; E\|500; E\rangle$	$\langle 500; A_1\|500; E\rangle$
v_0	9841.088(17)	9841.185(12)	–
B	3.5627(23)	3.5609(15)	–
C	3.3757(25)	3.3546(16)	–
D_J	−0.000773(51)	−0.000668(31)	–
$r_{\rm eff}$	–	−0.11005(20)	–
$q_{\rm eff}$	–	−0.2467(31)	–
$q_{\rm eff}^{J}$	–	0.000364(87)	–
$B\Omega\zeta_{\rm eff}^{y}$	–	–	−0.0136(15)
$\alpha_{\rm eff}^{BC}$	–	–	0.0599(34)
$\alpha_{\rm eff}^{BC,J}$	–	–	0.00484(10)
$\alpha_{\rm eff}^{BB}$	–	–	−0.0143(27)
$\alpha_{\rm eff}^{BB,J}$	–	–	−0.014122(83)
$\alpha_{\rm eff}^{BB,K}$	–	–	−0.00049(11)
$\sigma \times 10^{-2}$		2.99	

Table 2. Energy levels (cm^{-1}) of the (500; A_1) and (500; E) local mode states of AsH_3.

J	K	Sym.of vib.	Sym.	Obs.	Cal.	Cal.-Obs.	$N^{(a)}$
0	0	$1^{(b)}$	$0^{(c)}$	9841.068	9841.088	−0.020	1
0	0	2	2	9841.181	9841.184	−0.003	1
1	1	2	0	9848.342	9848.349	−0.007	1
1	0	1	1	9848.270	9848.236	0.034	2
1	1	2	1	9847.815	9847.836	−0.021	2
1	1	1	2	9848.016	9848.034	−0.018	2
1	0	2	2	9848.549	9848.534	0.015	1
1	1	2	2	9847.871	9847.872	−0.001	1
2	0	1	0	9863.168	9863.150	0.018	2
2	1	2	0	9862.342	9862.356	−0.014	2
2	2	2	0	9860.323	9860.368	−0.045	2
2	1	2	1	9863.951	9863.909	0.042	1
2	2	2	1	9860.895	9860.941	−0.046	2
2	1	1	2	9861.913	9861.940	−0.027	2
2	2	1	2	9861.741	9861.708	0.033	2
2	0	2	2	9863.256	9863.214	0.042	1
2	1	2	2	9862.516	9862.537	−0.021	3
2	2	2	2	9861.347	9861.340	0.007	2
3	3	1	0	9882.252	9882.208	0.044	2
3	1	2	0	9886.657	9886.660	−0.003	3
3	2	2	0	9881.847	9881.846	0.001	2
3	0	1	1	9885.640	9885.620	0.020	2
3	3	1	1	9880.551	9880.580	−0.029	1
3	1	2	1	9882.020	9882.067	−0.047	2
3	2	2	1	9883.544	9883.491	0.053	3
3	1	1	2	9882.702	9882.765	−0.063	2
3	2	1	2	9883.100	9883.172	−0.072	3
3	0	2	2	9886.255	9886.213	0.042	2
3	1	2	2	9885.258	9885.267	−0.009	3
3	2	2	2	9883.635	9883.616	0.019	5
3	3	2	2	9879.760	9879.732	0.028	4
3	3	2	2	9881.540	9881.513	0.027	1
4	0	1	0	9916.519	9916.515	0.004	2
4	3	1	0	9912.376	9912.359	0.017	1
4	1	2	0	9909.737	9909.722	0.015	1
4	2	2	0	9907.020	9907.031	−0.011	3
4	4	2	0	9909.301	9909.275	0.026	3
4	3	1	1	9911.198	9911.214	−0.016	2
4	1	2	1	9917.265	9917.268	−0.003	1
4	2	2	1	9910.302	9910.313	−0.011	2
4	4	2	1	9908.232	9908.243	−0.011	1
4	1	1	2	9905.408	9905.413	−0.005	3
4	2	1	2	9906.639	9906.587	0.052	2
4	4	1	2	9909.075	9909.087	−0.012	1
4	0	2	2	9917.257	9917.265	−0.008	2
4	1	2	2	9916.676	9916.660	0.015	3
4	2	2	2	9912.869	9912.903	−0.034	2
4	3	2	2	9909.988	9909.951	0.037	3
4	3	2	2	9913.878	9913.863	0.015	2
4	4	2	2	9910.338	9910.267	0.071	3
5	3	1	0	9937.758	9937.756	0.002	3
5	1	2	0	9956.870	9956.892	−0.022	1
5	2	2	0	9943.428	9943.471	−0.043	2
5	4	2	0	9951.128	9951.117	0.011	2
5	5	2	0	9946.252	9946.242	0.010	1
5	0	1	1	9956.947	9956.952	−0.005	3

Table 2. (*Continued*)

J	K	Sym.of vib.	Sym.	Obs.	Cal.	Cal.-Obs.	$N^{(a)}$
5	3	1	1	9951.830	9951.849	−0.019	1
5	1	2	1	9942.373	9942.398	−0.025	4
5	2	2	1	9937.530	9937.540	−0.010	1
5	4	2	1	9947.942	9947.984	−0.042	5
5	5	2	1	9940.363	9940.347	0.016	1
5	1	1	2	9938.557	9938.594	−0.037	3
5	2	1	2	9939.439	9939.435	0.004	1
5	4	1	2	9945.748	9945.735	0.013	4
5	5	1	2	9942.444	9942.495	−0.051	3
5	0	2	2	9957.153	9957.172	−0.019	3
5	1	2	2	9957.081	9957.091	−0.010	2
5	2	2	2	9950.554	9950.541	0.013	2
5	3	2	2	9943.340	9943.335	0.005	2
5	3	2	2	9951.953	9951.953	−0.000	2
5	4	2	2	9944.825	9944.849	−0.024	2
5	5	2	2	9941.999	9941.940	0.059	1
6	0	1	0	10007.712	10007.700	0.012	2
6	3	1	0	10000.807	10000.830	−0.023	2
6	6	1	0	9981.160	9981.178	−0.018	3
6	1	2	0	9978.007	9978.011	−0.004	1
6	2	2	0	9976.277	9976.266	0.011	1
6	4	2	0	9993.436	9993.421	0.015	5
6	5	2	0	9983.737	9983.767	−0.030	1
6	3	1	1	9981.451	9981.425	0.026	1
6	6	1	1	9985.175	9985.141	0.034	1
6	1	2	1	10006.847	10006.878	−0.031	1
6	2	2	1	9989.894	9989.883	0.011	2
6	4	2	1	9998.094	9998.083	0.011	2
6	5	2	1	9977.414	9977.396	0.018	2
6	1	1	2	9976.214	9976.204	0.010	3
6	2	1	2	9977.285	9977.315	−0.030	2
6	4	1	2	9981.246	9981.231	0.015	3
6	5	1	2	9980.570	9980.599	−0.029	3
6	0	2	2	10007.595	10007.592	0.003	1
6	1	2	2	10007.238	10007.204	0.034	3
6	2	2	2	9997.897	9997.882	0.015	2
6	3	2	2	9988.657	9988.661	−0.004	1
6	3	2	2	9999.529	9999.528	0.001	4
6	4	2	2	9986.850	9986.825	0.025	3
6	5	2	2	9993.325	9993.349	−0.024	1
6	6	2	2	9978.224	9978.207	0.017	3
6	6	2	2	9984.364	9984.370	−0.006	2

(a) N is the number of assigned transitions of the energy levels. (b) 1 denotes A_1 and 2 denotes E. (c) 0, 1, 2 denote A_1, A_2 and E, respectively.

V. DISCUSSION

The agreement between calculations and observations of the effective vibration-rotational parameters is satisfactory in the (300) and (400) overtones,[11,13−15] indicating weak interactions such as the Fermi resonances between the stretching and bending vibrations. However, the result of this work shows that the observed band origins of the (500) local mode pairs are about $4\,cm^{-1}$ lower than the calculated values indicating vibrational perturbations. Significant discrepancies between the calculated and observed H_{22}-type constants are also found in the (500) overtone. These predictions of H_{22}-type constants are not listed in this paper. We believe that the discrepancies are due to the rotational perturbations which are not considered in the present analysis.

It is of interest to investigate the rotational structure of the $(n00)$ $(n = 1, 2, \cdots, 6)$ overtones. Figure 2 demonstrates the evolution of the $J = 3$ levels in these overtones. It can be seen that the rotational structure of the (100) state which corresponds to the normal

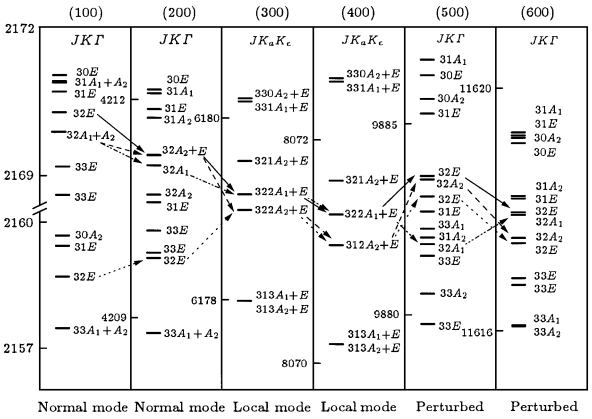


Fig.2. Diagram of $J = 3$ rotational level pattern of AsH_3 $(n00)$ $(n = 1, 2, \cdots, 6)$ vibrational states. The energy level data are taken from Ref.[11–14] and this work. The arrows show the evolution of the rotational levels with the same K values from the normal mode to local mode limit, and the effects of perturbations in higher overtones.

mode limit exhibits typical symmetric top characters, and K is a good quantum number to label the levels (as we have done in Fig.2). The rotational levels of the (200) state are also labeled by the K quantum number since the (200) state is closer to the normal mode than the local mode limit. Due to the Darling-Dennison resonances, the local mode pairs (the lowest A_1 and E states within each stretching manifold) become degenerated at high vibrational excitation and the spectra show complicated rotational structures. In the (300) and (400) states which are close to the local mode limit, the symmetric top reduces to the asymmetric top. When J is not high, the energy levels with the same K become degenerated. K is a quasi-good quantum number, and corresponds to the asymmetric top quantum number K_c in the asymmetric top model. The asymmetric top quantum numbers J, K_a and K_c are used to label the levels in the (300) and (400) states in Fig.2. The symmetry of the levels is also given in the C_{3v} point group. From Fig.2, we can see that each level of E symmetry is degenerated with one level of A_1 or A_2 symmetry. However, this local mode feature is destroyed by perturbations in the (500) and (600) states. The rotational level pattern withdraw to that of the normal mode character and should be labeled with the symmetric top K quantum number again.

It has been pointed out that although the bending fundamentals of AsH_3 are below half of the stretching fundamentals, the Fermi resonances between the stretching and bending vibrations may be important at high vibrational excitations due to the large stretching anharmonicity.[13,16] Particularly, the perturbation from the $(400+2v_2)$ state, which involves one local mode pairs and double bending excitation modes, is considered important in our study. A further investigation will be carried out with a global fit with the rotational energy levels obtained from the recorded high resolution spectra including the bending modes.

ACKNOWLEDGMENTS

Oleg N. Ulenikov thanks University of Science and Technology of China in Hefei for the visiting professorship during May-June, 1998. Lin Hai thanks Dr. Wang Xiao-gang for helpful discussion.

REFERENCES

[1] M. S. Child, L. Halonen, *Adv. Chem. Phys.*, **57**(1984), 1.
[2] L. Halonen, A. G. Robiette, *J. Chem. Phys.*, **84**(1986), 6861.
[3] K. K. Lehmann, *J. Chem. Phys.*, **95**(1991), 2361.
[4] K. K. Lehmann, *J. Chem. Phys.*, **96**(1992), 7402.
[5] Q. S. Zhu, *Spectrochim. Acta*, **A48**(1992), 193.
[6] T. Lukka, L. Halonen, *J. Chem. Phys.*, **101**(1994), 8380.
[7] X. G. Wang, Q. S. Zhu, *J. Chem. Phys.*, **105**(1996), 8011.
[8] Q. S. Zhu *et al., Chem. Phys. Lett.*, **150**(1988), 181.
[9] M. Halonen *et al., J. Chem. Phys.*, **95**(1991), 7099.
[10] M. Halonen *et al., Chem. Phys. Lett.*, **203**(1993), 157.
[11] O. N. Ulenikov *et al., J. Chem. Phys.*, **105**(1996), 7310.
[12] S. F. Yang *et al., Spectrochim. Acta*, **A53**(1997), 157.
[13] J. X. Han *et al., Spectrochim. Acta*, **A53**(1997), 1705.
[14] J. X. Cheng *et al., Chinese Phys. Lett.*, **14**(1997), 656.
[15] J. X. Cheng *et al., Spectrochim. Acta*, **A54**(1998), 1947.
[16] M. Halonen *et al., J. Phys. Chem.*, **96**(1992), 4225.
[17] T. Lukka *et al., J. Chem. Phys.*, **102**(1995), 5200.
[18] H. Lin *et al., J. Mol. Spectrosc.*, **187**(1998), 89.
[19] S. F. Yang *et al., J. Chem. Soc. Faraday Trans.*, **94**(1998), 1397.
[20] D. Wang *et al., Spectrochim. Acta*, **55**(1999), 109.
[21] J. P. Chevillard *et al., Can. J. Phys.*, **67**(1989), 1065.
[22] C. Di Lauro, I. M. Mills, *J. Mol. Spectrosc.*, **21**(1966), 386.
[23] G. Tarrago *et al., J. Mol. Spectrosc.*, **178**(1996), 10.